The structural composition of soil phosphomonoesters as determined by solution 31P NMR spectroscopy and transverse relaxation (T2) experiments

Author(s):
McLaren, Timothy I.; Verel, René; Frossard, Emmanuel

Publication date:
2019-07

Permanent link:
https://doi.org/10.3929/ethz-b-000333449

Originally published in:
Geoderma 345, https://doi.org/10.1016/j.geoderma.2019.03.015

Funding acknowledgement:
169256 - Identifying the chemical nature of organic phosphorus in soil extracts with increasing molecular weight (SNF)

The structural composition of soil phosphomonoesters as determined by solution ^{31}P NMR spectroscopy and transverse relaxation (T_2) experiments

Timothy I. McLaren[a,*], René Verel[b] and Emmanuel Frossard[a]

[a] Department of Environmental Systems Science, ETH Zurich, CH-8315 Lindau, Switzerland

[b] Department of Chemistry and Applied Biosciences, ETH Zurich, CH-8093 Zurich, Switzerland

[*] Corresponding author, email: timothy.mclaren@usys.ethz.ch

Corresponding author

[*]Phone: +41 52 354 91 49, email: timothy.mclaren@usys.ethz.ch

Abstract: In terrestrial ecosystems, a large proportion of the phosphorus (P) in soil is often found within soil organic matter. However, the majority of organic P in soil remains 'unresolved' and is largely observed as a 'broad' signal within the phosphomonoester region of a solution ^{31}P nuclear magnetic resonance (NMR) spectrum on soil extracts. Our aim was to gain insight into the composition of four soils using the transverse relaxation (T_2) time of the magnetisation in solution ^{31}P NMR spectroscopy as a probe of their structure. We found the broad signal within the phosphomonoester region rapidly decayed compared to the sharp signals (i.e. *myo*- and *scyllo*-inositol hexakisphosphate) across all soils, which corresponded to the former having a shorter T_2 time than the latter, and supports the existence of a broad signal due to supra-/macro-molecular structures. Furthermore, measures of the broad signal's line-width at half peak intensity based on T_2 times were found to be less than that obtained from spectral deconvolution fitting. Therefore, our results strongly suggest that the broad signal is itself comprised of more than one component. The significance of this is that the chemical nature of a large proportion of soil organic P appears to be structurally complex.

1. Introduction

Soil organic matter is an essential component of terrestrial ecosystems because of its critical role in providing ecosystem services (Schmidt et al., 2011). Phosphorus (P) is an innate constituent of soil organic matter (Kirkby et al., 2011), however, a large proportion (typically > 50 %) of the organic P in soil remains 'unresolved' (Jarosch et al., 2015; McLaren et al., 2015a). This pool has so far not been directly attributed to recognisable biomolecules (Bünemann et al., 2008a; Noack et al., 2012), but largely described as comprising of phosphomonoesters (McLaren et al., 2015a), associated with large molecular weight material (Jarosch et al., 2015; McLaren et al., 2015a; Steward and Tate, 1971), 'humic acid' fractions (Bedrock et al., 1994; He et al., 2006), and soil organic matter (Condron and Goh, 1989; McLaren et al., 2014; Swift and Posner, 1972). New insight is needed on the chemical nature of this unresolved pool of soil organic P, which will improve our understanding of the P cycle in soil-plant systems (George et al., 2018).

Solution ^{31}P nuclear magnetic resonance (NMR) spectroscopy on alkaline extracts has been the predominant method used to identify the chemical nature of soil organic P since 1980 (Cade-Menun and Liu, 2014; Newman and Tate, 1980). The main classes of organic P detected in soil extracts are phosphomonoesters ($ROPO_3^{2-}$: where R is an organic moiety), phosphodiesters ($R_1OR_2OPO_2^-$: where R_1 and R_2 are organic moieties), and phosphonates (e.g. $RPO(OH)_2$, where R is an organic moiety) (Condron et al., 2005). In general, the majority of organic P (typically > 80 %) occurs as phosphomonoesters in soil extracts (Condron et al., 2005). However, due to a high degree of signal overlap within this region of a NMR spectrum, spectral deconvolution fitting procedures are required to partition the NMR signal and assign peaks to various compounds of organic P (Doolette and Smernik, 2015). The problem with this is that there are differing views on how to apply spectral deconvolution fitting procedures to solution ^{31}P NMR spectra on soil extracts (Doolette and Smernik, 2015), which results in considerable differences in the reported distribution and concentrations of 'identified' soil organic P.

There are two main approaches of applying spectral deconvolution fitting procedures to the phosphomonoester region. These are: 1) the deconvolution fitting procedure of Turner et al. (2003) or modifications therefore (i.e. Hill and Cade-Menun (2009) and Vincent et al. (2012)), which involve fitting a series of 'sharp' peaks from the peak maxima to the baseline of the spectra within the phosphomonoester region; and 2) the deconvolution fitting procedure of Bünemann et al. (2008b) or

modifications therefore (i.e. McLaren et al. (2015b)), which involves fitting a 'broad' (or 'background') peak and then any 'sharp' overlying peaks. There is strong evidence to include a broad peak when carrying out spectral deconvolution fitting based on (i) an overestimation of concentrations of *myo*-inositol hexakisphosphate (*myo*-IHP) if a broad signal is not included (Doolette et al., 2010; Doolette et al., 2011), (ii) preferential extraction of *myo*-IHP with hydrofluoric acid, which reveals NMR signal at the chemical shifts of *myo*-IHP but within an underlying broad signal (Dougherty et al., 2007), (iii) concentrations of organic P that were not hydrolysable by enzymes in NaOH-EDTA extracts were related to that of the broad signal and also organic P in large molecular weight (> 5 kDa) fractions (Jarosch et al., 2015), and (iv) the isolation of the broad signal in large molecular weight fractions (> 10 kDa) (McLaren et al., 2015a). However, the structural composition of the broad signal is itself not known and could be described as (i) a series of neighbouring sharp peaks that merge to visually appear as a broad peak or (ii) one (or a few) large and complex supra-/macro-molecules that exhibit a broad peak (Levitt, 2008).

Compounds have several different types of relaxation properties under NMR conditions, which have previously been explained in detail (Bloembergen et al., 1948; Claridge, 2016; Keeler, 2010; Levitt, 2008). Transverse relaxation (T_2) experiments can probe the underlying structure of a NMR signal as comprising of 'broad' and 'sharp' components (Claridge, 2016; Keeler, 2010; Levitt, 2008; Meiboom and Gill, 1958; Schmidt-Rohr and Spiess, 1994). This is based on probing their T_2 times, which are generally related to a compound's line-width at half peak intensity (Bloembergen et al., 1948; Claridge, 2016). Essentially, T_2 relaxation provides information on the dynamics of molecules as probed by the coherence lifetime of their spin magnetisation in the transverse plane (x-y plane). This distinguishes the effects of line-broadening due to variations within the magnetic field caused by instrumental imperfections or slight conformational variations, in which case a broad signal would comprise a series of sharp neighbouring peaks (i.e. 'inhomogeneous' broadening) (Levitt, 2008). In contrast, variations within the magnetic field caused by differences in the molecular dynamics of compounds can be quantified based on their T_2 properties, in which case a broad signal would comprise of a single (or a few) compounds (i.e. 'homogeneous' broadening) (Levitt, 2008). See Figure 3.24 in Schmidt-Rohr and Spiess (1994) for a graphical representation on the structural composition of line-broadening. In general, compounds with relatively slow molecular motion tend to be of larger molecular weight and have shorter T_2 times (i.e. 'broad' line-widths), whereas compounds with

relatively fast molecular motion tend to be of smaller molecular weight and have longer T_2 times (i.e. 'sharp' line-widths) (Bloembergen et al., 1948; Keeler, 2010). Therefore, T_2 experiments can preferentially 'filter' out NMR signal from 'broad' components to that of 'sharp' components based on differences in their T_2 times (Keeler, 2010).

Here, for the first time, we carry out solution ^{31}P NMR spectroscopy with T_2 experiments on soil extracts to determine the structural composition of soil phosphomonoesters. We hypothesised that a broad signal would preferentially decay to that of sharp signals (i.e. *myo*-IHP and *scyllo*-inositol hexakisphosphate (*scyllo*-IHP)) in the phosphomonoester region based on differences in their T_2 times.

2. Materials and methods

2.1 Soil information

Two soils of the mineral (Ah) horizon under forest were sourced from the "Ecosystem Nutrition: Forest Strategies for limited Phosphorous Resources (SPP 1685)" project in Germany (Lang et al., 2017). The two soils collected in 2015 from the Bad Brückenau (BBR) and Vessertal (VES) sites are classified as Cambisols (IUSS Working Group WRB, 2015), which were developed on basalt and trachyandesite parent material, respectively. At each site, the litter layer was removed and approximately 5 cores were sampled of the horizon within an area of 4 m^2 and bulked. The soil was then sieved at field moisture to pass through a 5 mm sieve and then stored at 4 °C. In 2016, a 200 g subsample of moist soil was removed and dried in a laboratory oven at 40 °C for two weeks. The long-term cool storage of moist samples appear to have a minor effect on the distribution of total organic P (Cade-Menun et al., 2005), and concentrations of total organic P in soil from these sites are similar to those reported in previous studies (Bünemann et al., 2016; Lang et al., 2017). A soil under cropping was collected from the 0 – 10 cm layer of the experimental plot (the conventional 1.4 LU ha^{-1} + mineral fertiliser treatment) of the long-term "bio-Dynamic, bio-Organic, and "Konventionell" (DOK)" field experiment in Switzerland (Keller et al., 2012). The soil was collected in 2015 and is classified as a Luvisol (IUSS Working Group WRB, 2015), which was developed from fluvioglacial deposits. Details of soil collection and preparation are similar to that described in Keller et al. (2012). Lastly, the reference soil (1BS102M – Elliot) of the International Humic Substances Society was purchased in 2016. The soil was originally collected from the 0 – 20 cm layer of a native grassland in the United States and is classified as a Chernozem (IUSS Working Group WRB, 2015). Details of soil collection

and preparation have been previously described (IHSS, 2013). Some basic chemical properties of the soils used in this study are reported in Table 1.

[Suggested location of Table 1]

2.2 Extraction of soil organic phosphorus

Soil organic P was extracted based on the method of Cade-Menun et al. (2002). Briefly, 4 g of soil was extracted with 40 mL of 0.25 M NaOH + 0.05 M Na_2-EDTA solution on a horizontal shaker at 160 rpm for 16 hours. The extracts were then centrifuged at 5000 rpm for 20 minutes, and the supernatant passed through a Whatman no. 42 filter paper. A 20 mL aliquot of the filtrate was frozen at -80 °C, and then lyophilised and weighed (Doolette et al., 2010). This resulted in 612 to 835 mg of lyophilised material per tube across all soils. The lyophilised material was rapidly homogenised using a glass rod prior to subsampling and sample preparation for NMR analysis.

2.3 Preparation of lyophilised material for (1D) nuclear magnetic resonance spectroscopy

Preparation of lyophilised material for solution ^{31}P NMR analyses was based on a modification of Vincent et al. (2012), except in this study the lyophilised material was dissolved with NaOH-EDTA solution (Spain et al., 2018). Briefly, 150 mg of lyophilised material was weighed into a 1.5 mL microcentrifuge tube, which was dissolved in 600 µL of 0.25 M NaOH + 0.05 M Na_2-EDTA solution. The tube was then vortexed for 2 minutes, left to stand for several hours to allow for complete hydrolysis of RNA and phospholipids (Doolette et al., 2009; Vestergren et al., 2012), and then centrifuged at 10000 rpm for 20 minutes. A 500 µL aliquot of the supernatant was transferred to another 1.5 mL microcentrifuge tube, which was then spiked with a 50 µL aliquot of 32.4 mM methylenediphosphonic acid in a D_2O matrix (MDP: Sigma-Aldrich, M9508) and 50 – 100 µL of sodium deuteroxide solution 40 wt. % in D_2O (NaOD: Sigma-Aldrich, 372072). The tube was then vortexed for 10 seconds and transferred to a 5 mm NMR tube prior to analysis.

2.4 Solution phosphorus-31 nuclear magnetic resonance spectroscopy with transverse relaxation (T_2) experiments

All spectra were obtained with a Bruker Avance III HD 500 NMR spectrometer (Bruker Corporation; Billerica, MA) at the NMR facility of the Laboratory of Inorganic Chemistry (Hönggerberg, ETH Zürich). The NMR spectrometer was set at a ^{31}P frequency of 202.5 MHz with inverse gated broadband proton decoupling and a 90° pulse of 14 μs duration. Solution ^{31}P NMR spectroscopy with a Carr-Purcell-Meiboom-Gill (CPMG) pulse sequence was carried out on all samples (Meiboom and Gill, 1958).

The transverse relaxation (T_2) experiment involved a 90º pulse to cause magnetisation of ^{31}P nuclei from the z-axis to the x–y plane in which the nuclei spin is perpendicular to the magnetic field (M_τ). The ^{31}P nuclei immediately begin to return to their equilibrium state as they fan out in the x–y plane caused by the sum contribution of any homogenous and inhomogeneous broadening. A 180º pulse is applied after a spin-echo delay (τ) to invert the magnetisation of ^{31}P nuclei in the x–y plane, which corrects for any effects arising from inhomogeneity caused by the magnetic field. After a second spin-echo delay (τ) in which the ^{31}P nuclei has been refocused in the x–y plane (i.e. the opposite direction to that initially induced by the 90º pulse), the free induction decay in the x–y plane is recorded. See Figures 2.27 (c) and 2.28 in Claridge (2016) for a graphical representation of the CPMG pulse sequence and a vector diagram of the spin dynamics, respectively. Briefly, the experiment used a constant spin-echo delay (τ) of 5 ms, and the spin-echo period was repeated for a total of eight iterations (total spin-echo period at each iteration: 5, 50, 100, 150, 200, 250, 300, and 400 ms). A total of 1024 scans was obtained at each spin-echo period. A recycle delay of 4 seconds was used prior to the 90º pulse. A preliminary inversion recovery experiment (Vold et al., 1968) revealed the longest recycle delays occurred for that of orthophosphate across all soils, ranging from 4.5 to 20.6 seconds (Table 2). Therefore, a recycle delay of 4 seconds for the T_2 experiment is shorter than that indicated for complete relaxation between pulses, which would be required for obtaining quantitative 1D spectra (i.e. for calculations on a soil-weight basis: mg P kg^{-1}). However, this is not a problem for the determination of T_2 times because recycle delays remain constant across all eight iterations of the T_2 experiment.

[Suggested location of Table 2]

185 The total duration of the T_2 experiment for each soil was approximately 13 hours. However,
186 due to poor spectral resolution at the last time spin-echo period (400 ms), a second experiment was
187 carried out with 4096 scans at two spin-echo periods (5 and 400 ms), and again a third experiment with
188 16384 scans at one spin-echo period (400 ms). These experiments provide NMR spectra with a greater
189 signal-to-noise ratio at the shortest and longest spin-echo periods (5 and 400 ms), compared to the full
190 experiment across eight spin-echo periods, in order to assess visually any differences in decaying
191 components. The total duration of these T_2 experiments for each soil was approximately 12 and 24
192 hours, respectively.
193 All spectra were initially processed within TopSpin® software (Bruker Corporation; Billerica,
194 MA). The spectra were phased and baseline corrected, and defined integral ranges were established
195 according to the presence of ^{31}P NMR signal. In general, this occurred in the phosphonate region (δ ~
196 20.0 to 19.8 ppm, 18.5 to 18.0 ppm, and 17.3 to 16.3 ppm), the combined orthophosphate and
197 phosphomonoester region (δ ~ 5.7 to ~ 2.8 ppm), the phosphodiester region (δ ~ -0.6 to ~ -1.6 ppm)
198 and the pyrophosphate region (δ ~ -4.3 to ~ -4.6 ppm). These integrals were then used to calculate their
199 T_2 times (ms) using Equation 1, except for that of the combined orthophosphate and phosphomonoester
200 region. Spectral deconvolution fitting procedures was carried out in this region using Matlab (The
201 MathWorks Inc.; Natick, MA) in order to partition the signal based on the method of Bünemann et al.
202 (2008b). The spectral deconvolution procedures were implemented through custom Matlab scripts
203 incorporating functions from the MatNMR Toolbox (van Beek, 2007) for the import of spectral data
204 and using a modified version of the peakfit Toolbox (version 8.3) by Tom O'Haver for the nonlinear
205 least squares fitting of the experimental data. The T_2 times of the partitioned NMR signals were then
206 calculated using Equation 1. This included obtaining the T_2 times of orthophosphate, the broad signal,
207 the individual *myo*-IHP peaks, and also that of the combined peaks of *myo*-IHP, and *scyllo*-IHP.
208

209 $$M_\tau = M_o \times \exp^{\left(\frac{-\tau}{T_2}\right)}, \quad (1)$$

210 where 'M' refers to the net magnetisation derived from the average angular momentum of all spinning
211 nuclei in the x–y plane, 'τ' refers to the spin-echo delay in milliseconds (ms), and 'T_2' refers to the
212 transverse relaxation time (ms).
213

The structural composition of the broad signal can be further probed by comparing measures of its line-width at half peak intensity ($W_{1/2}$) based on spectral deconvolution and T_2 times. Measures of $W_{1/2}$ are normally obtained directly from NMR spectra or spectral deconvolution fitting but can also be calculated using Equation 2 based on T_2 times. The purpose of this was to ascertain if the calculated $W_{1/2}$ of the broad peak based on spectral deconvolution was equal or greater than that based on T_2 times. If measures of $W_{1/2}$ of the former were greater than that of the latter then this would indicate the broad signal is comprised of more than one component.

$$W_{1/2} = \frac{1}{(\pi \times T_2)} \ , \qquad (2)$$

where '$W_{1/2}$' refers to a peak's line-width at half peak intensity and 'T_2' refers to the transverse relaxation time (ms).

2.5 Graphics and statistical analyses

All graphics and statistical analyses (standard error of the model coefficient) were carried out using R 3.2.0 (R Core Team, 2016). In Figure 1, solution ^{31}P NMR spectra obtained with a CPMG sequence at a spin-echo period of 5 ms (black line) and 400 ms (blue line) was taken from the 4096 and 16384 scans, respectively.

3. Results and discussion

3.1 Soil extraction and solution phosphorus-31 nuclear magnetic resonance spectra

The four soils used in this study were chosen for differences in their chemical properties and distribution of soil organic P (Table 1). Concentrations of total P ranged from 1202 and 3793 mg kg^{-1} across all soils based on laboratory X-ray fluorescence (LXRF). Pools of total P in NaOH-EDTA extracts ranged from 309 to 1612 mg kg^{-1} across all soils. The extraction efficiency of total P by NaOH-EDTA ranged from 26 to 42 % of the total soil P by LXRF, which is consistent with previous studies (McLaren et al., 2015a; Missong et al., 2016). Soil BBR and VES had greater concentrations of soil organic P and total carbon and nitrogen than in the DOK and Elliot soils. However, the BBR soil had more than eight times the concentration of oxalate extractable iron compared to that of the VES soil. Concentrations of oxalate extractable iron have been found to be correlated with that of inositol phosphates (Turner et al., 2003; Vincent et al., 2012). Also, the Elliot soil had three times the

concentration of total carbon and more than twice the concentration of oxalate extractable iron compared to the DOK soil.

Solution ^{31}P NMR spectra on all soil extracts were highly resolved and show the majority of NMR signal in the orthophosphate and phosphomonoester region. Solution ^{31}P NMR spectra of the BBR and VES soils reveal prominent NMR signals due to *myo*-IHP and *scyllo*-IHP relative to those in the DOK and Elliot soils. Based on a visual assessment, all soils had a broad signal that lies underneath the sharp signals (Doolette and Smernik, 2015), which is particularly evident in the DOK and Elliot soils. Therefore, the proportion of sharp peak (*myo*-IHP and *scyllo*-IHP) intensity relative to the broad peak intensity varied across all soils.

3.2 Transverse relaxation (Carr-Purcell-Meiboom-Gill) experiments

Solution ^{31}P NMR spectra with the shortest (5 ms) and longest (400 ms) spin-echo period of the orthophosphate and phosphomonoester region are shown in Figure 1. The T_2 experiments of all soils revealed a fast decaying broad component relative to that of *myo*-IHP and *scyllo*-IHP in the phosphomonoester region, which was particularly evident in the BBR soil. The existence of a fast decaying broad component indicates the presence of phosphomonoesters that have a slow molecular motion and a large molecular weight (Bloembergen et al., 1948; Levitt, 2008). These results support previous studies that have demonstrated the existence of organic P in large molecular weight fractions (Jarosch et al., 2015; McLaren et al., 2015a; Steward and Tate, 1971; Thomas and Bowman, 1966). McLaren et al. (2015a) investigated the chemical nature of organic P in soil extracts from five different soil types that had been separated into 'small' (< 10 kDa) and 'large' (> 10 kDa) molecular weight fractions using ultrafiltration devices and solution ^{31}P NMR spectroscopy. The authors found the chemical nature of organic P in the large molecular weight fraction (> 10 kDa) was markedly different to that of the small molecular weight fraction (< 10 kDa). The former was dominated by a broad signal whereas the latter contained considerably less broad signal than the 'unfractionated' extracts.

The decay of the broad component in the phosphomonoester region was similar across all soils, which shows its composition is due to 'homogeneous' line-broadening (Figure 1). However, the decay of the broad signal appears to be visually greater in the δ 4.5 ppm region compared to that in the δ 4.0 ppm region across most soils, which indicates more than one component of the broad signal and the presence of a few adjacent Lorentzian/Gaussian distributions. Spectral deconvolution fitting

procedures based on the method of Bünemann et al. (2008b) have typically involved a single Lorentzian/Gaussian distribution when accounting for the broad signal, but in some cases, this has included two adjacent Lorentzian/Gaussian distributions (McLaren et al., 2015b). Nevertheless, our data supports the fitting of a Lorentzian/Gaussian distribution with a broad line-width in order to account for the total broad signal that lies underneath the sharp signals in the phosphomonoester region.

In addition to the broad signal, there were some sharp signals that rapidly decayed concomitant with the broad signal, particularly that at ~ δ 4.5 ppm (Figure 1). Whilst this signal would be considered to have a relatively slow decay due to its narrow line-width, the peak is similar to that reported in large molecular weight fractions (> 10 kDa) by McLaren et al. (2015a). Its presence has also been suggested in unfractionated soil extracts (Cade-Menun et al., 2018). Our results support its association with organic P in large molecular weight fractions and suggest that it should be considered in relation to the broad signal.

No study has investigated the structural composition of phosphomonoesters in mineral soils. However, Vincent et al. (2012) attempted to understand this for an Oa horizon of an Oxyaquic Haplocryod (Soil Survey Staff, 1992) under boreal forest using solution ^{31}P NMR spectroscopy with transverse relaxation ($T_{1\rho}$, i.e. decay time constant for transverse relaxation in the presence of a rotating frame field) (Levitt, 2008). The technique is similar to that of T_2 experiments (as measured by a CPMG sequence) for measurements of transverse relaxation times, except the former uses a 90º pulse to cause magnetisation of ^{31}P nuclei from the z-axis to the x–y plane and remain in the same direction of transverse magnetization using a constant radiofrequency pulse or "spin-lock" pulse with increasing durations. Based on the reported experimental setup, the authors found no difference in the solution ^{31}P NMR spectra of one soil extract at a short (0.1 ms) and a longer (32 ms) spin-lock duration for a spin-lock pulse with an amplitude of 3.0 kHz. This finding is in contrast with the current study that clearly shows a fast decaying 'broad' component in the phosphomonoester region. A possible reason for this is that the spin-lock durations used in the study of Vincent et al. (2012) were too short to allow sufficient separation of the broad and sharp components.

[Suggested location of Figure 1]

Solution ^{31}P NMR spectroscopy with T_2 experiments demonstrated the existence of a broad signal that lies underneath the sharp signals within the phosphomonoester region of NMR spectra. Therefore, spectral deconvolution fitting procedures based on the method of Bünemann et al. (2008b) was applied in order to determine the T_2 times of various P species. The absolute T_2 values for each P species differed greatly between soils. This is unsurprising given the strong matrix effect that influences NMR properties such as differences in longitudinal relaxation (T_1) times and changes in chemical shifts, which is particularly the case in soil extracts (McDowell et al., 2006; Smernik and Dougherty, 2007). Indeed, factors affecting T_1 times are likely to affect T_2 times because the latter has been shown to be less (or in some cases equal to) than that of the former. Nevertheless, the relative differences in T_2 times between P species within each soil were generally consistent.

In general, T_2 times of the broad signal were considerably shorter than that for *myo*-IHP and *scyllo*-IHP (Table 3). Although, an accurate T_2 measure of *myo*-IHP was not possible in the Elliot soil due to its low concentration. The T_2 times of the *myo*-IHP peaks (C2, C1 and C3, C4 and C6, C5) were generally similar. The longest T_2 time of all organic P species was usually that of *scyllo*-IHP. Results for *myo*-IHP and *scyllo*-IHP are consistent with visual observations (Figure 1) and expected differences in T_2 values according to molecular motion/weight (McLaren et al., 2015a; Wang et al., 2017).

The T_2 times obtained from the CPMG experiment place a limit on the homogeneous line-width of the broad signal. Calculation of $W_{1/2}$ based on spectral deconvolution fitting was on average 196 Hz across all soils. In contrast, measures of $W_{1/2}$ based on T_2 times were on average 11 Hz across all soils. Whilst T_2 experiments support the broad signal as being caused by homogenous broadening relative to the overlying sharp signals, a comparison of its calculated $W_{1/2}$ suggest that the broad signal is itself comprised of more than one component.

Solution ^{31}P NMR spectroscopy with T_2 experiments also provided some insight on other forms of organic P in soil extracts. Phosphodiesters (i.e. DNA) rapidly decayed and had short T_2 times (Table 3). This is consistent with the NMR signal of DNA being broad and contained in large molecular weight fractions (> 10 kDa) (McLaren et al., 2015a; Wang et al., 2017). The T_2 time of 2-aminoethylphosphonate, and an unknown phosphonate, was long in the VES soil, which is expected given its small molecular weight (< 1 kDa). In contrast, this was relatively short in the BBR and it is unclear why this was the case. A similar finding occurred for pyrophosphate and orthophosphate in this soil. Since the BBR soil contained large concentrations of soil organic matter and extractable metals, it

is possible that these forms are more associated with organic P in the broad signal, and/or there was an unknown matrix effect. It is also possible that T_1 times may have been influential as the T_1 times of MDP and orthophosphate in BBR were on average 54 % and 71 % less than for the other soils, respectively (Table 2).

[Suggested location of Table 3]

3.3 Implications

Soil organic matter is an important source of P to living organisms in terrestrial ecosystems. However, there is a paucity of knowledge on the chemical nature of soil organic P, particularly unresolved pools that typically comprise more than 50 % of the total pool of soil organic P (Dalal, 1977; Jarosch et al., 2015; McLaren et al., 2015a). For the first time, we reveal the structural composition of unresolved pools of soil organic P. Our results show that the majority of organic P in soil is in the form of large macro-/supra-molecular structures that is itself comprised of at least one component. This finding supports previous studies that show much of the organic P in soil is contained in large molecular weight fractions, and associated with humic acid fractions, which give rise to a predominantly broad NMR signal (He et al., 2006; Jarosch et al., 2015; McLaren et al., 2015a).

Historically, pools of soil organic P have largely been considered in isolation, whereby a specific form of organic P was the focus of a study (e.g. Turner et al. (2003)). The emerging view is that soil organic P contains structurally complex forms of organic P that are closely associated with the soil organic matter in addition to that of recognisable biomolecules (e.g. *myo*-IHP) (McLaren et al., 2015a). Whilst there is much research on the mechanisms associated with specific biomolecules of organic P, particularly that of *myo*-IHP (Turner et al., 2002), there is limited insight on the mechanisms governing pools of organic P as the broad signal in a NMR spectrum. There is supporting evidence to suggest their sequestration is related to factors affecting plant growth, soil organic matter and climate, which involve slow and soil-based mechanisms (Doolette et al., 2017; McLaren et al., 2017; Schefe et al., 2015).

Lastly, understanding the chemical nature of soil organic P often involves the use of solution ^{31}P NMR spectroscopy on soil extracts followed by spectral deconvolution fitting based on the method of Turner et al. (2003) or modifications thereof (Hill and Cade-Menun, 2009; Vincent et al., 2012).

However, we demonstrate that these methods do not take into account the existence of a broad peak, and will therefore likely result in an overestimation of sharp peaks within the phosphomonoester region, particular that of *myo*-IHP (Doolette et al., 2010). Consequently, studies that have reported concentrations of P species using deconvolution fitting procedures without an underlying broad peak may be unreliable. Clearly, the spectral deconvolution fitting method of Bünemann et al. (2008b) or modifications thereof (McLaren et al., 2015b), which includes a broad signal underneath the sharp signal within the phosphomonoester region, should be used for the quantification of all P species within this region. Given that the broad signal is a major pool of soil organic P, future research should be directed to further understand its composition and the mechanisms regulating its flux in soil.

Appendices – Supplementary material

None.

Acknowledgements

Financial support from Swiss National Foundation for Scientific Research is gratefully acknowledged (Project: 200021_169256). The authors would like to thank Dr Laurie Paule Schönholzer and Ms Doris Sutter for technical assistance. The authors are grateful to Dr Federica Tamburini, Dr Chiara Pistocchi, and Dr Astrid Oberson for providing soil samples. Lastly, we thank the anonymous reviewers who provided constructive feedback on the manuscript.

References

Bedrock, C.N., Cheshire, M.V., Chudek, J.A., Goodman, B.A., Shand, C.A., 1994. Use of 31P-NMR to study the forms of phosphorus in peat soils. Sci. Total Environ. 152 (1), 1-8.

Bloembergen, N., Purcell, E.M., Pound, R.V., 1948. Relaxation effects in nuclear magnetic resonance absorption. Physical Review 73 (7), 679-712.

Bünemann, E.K., Augstburger, S., Frossard, E., 2016. Dominance of either physicochemical or biological phosphorus cycling processes in temperate forest soils of contrasting phosphate availability. Soil Biol. Biochem. 101, 85-95.

392 Bünemann, E.K., Smernik, R.J., Doolette, A.L., Marschner, P., Stonor, R., Wakelin, S.A., McNeill,
393 A.M., 2008a. Forms of phosphorus in bacteria and fungi isolated from two Australian soils.
394 Soil Biol. Biochem. 40 (7), 1908-1915.
395 Bünemann, E.K., Smernik, R.J., Marschner, P., McNeill, A.M., 2008b. Microbial synthesis of organic
396 and condensed forms of phosphorus in acid and calcareous soils. Soil Biol. Biochem. 40 (4),
397 932-946.
398 Cade-Menun, B.J., Benitez-Nelson, C.R., Pellechia, P., Paytan, A., 2005. Refining 31P nuclear
399 magnetic resonance spectroscopy for marine particulate samples: Storage conditions and
400 extraction recovery. Marine Chemistry 97 (3), 293-306.
401 Cade-Menun, B.J., Elkin, K.R., Liu, C.W., Bryant, R.B., Kleinman, P.J.A., Moore, P.A., 2018.
402 Characterizing the phosphorus forms extracted from soil by the Mehlich III soil test.
403 Geochem. Trans. 19 (1), 7.
404 Cade-Menun, B.J., Liu, C.W., 2014. Solution phosphorus-31 nuclear magnetic resonance spectroscopy
405 of soils from 2005 to 2013: A review of sample preparation and experimental parameters. Soil
406 Sci. Soc. Am. J. 78 (1), 19-37.
407 Cade-Menun, B.J., Liu, C.W., Nunlist, R., McColl, J.G., 2002. Soil and litter phosphorus-31 nuclear
408 magnetic resonance spectroscopy J. Environ. Qual. 31 (2), 457-465.
409 Claridge, T.D.W., 2016. Chapter 2 - Introducing high-resolution NMR. In: T.D.W. Claridge (Ed.),
410 High-resolution NMR techniques in organic chemistry. Elsevier, Amsterdam, Nevtherlands,
411 pp. 11-59.
412 Condron, L.M., Goh, K.M., 1989. Molecular weight distribution of soil organic phosphorus under
413 irrigated pasture in New Zealand. J. Soil Sci. 40 (4), 873-878.
414 Condron, L.M., Turner, B.L., Cade-Menun, B., 2005. Chemistry and dynamics of soil organic
415 phosphorus. In: J.T. Sims, A.N. Sharpley (Eds.), Phosphorus: Agriculture and the
416 environment. ASA CSSA SSSA, Madison, Wisconsin USA.
417 Dalal, R.C., 1977. Soil organic phosphorus. Adv. Agron. 29, 83-117.
418 Doolette, A.L., Smernik, R.J., 2015. Quantitative analysis of 31P NMR spectra of soil extracts -
419 dealing with overlap of broad and sharp signals. Magn. Reson. Chem. 53 (9), 679-685.

Doolette, A.L., Smernik, R.J., Dougherty, W.J., 2009. Spiking improved solution phosphorus-31 nuclear magnetic resonance identification of soil phosphorus compounds. Soil Sci. Soc. Am. J. 73 (3), 919-927.

Doolette, A.L., Smernik, R.J., Dougherty, W.J., 2010. Rapid decomposition of phytate applied to a calcareous soil demonstrated by a solution 31P NMR study. Eur. J. Soil Sci. 61 (4), 563-575.

Doolette, A.L., Smernik, R.J., Dougherty, W.J., 2011. Overestimation of the importance of phytate in NaOH–EDTA soil extracts as assessed by 31P NMR analyses. Org. Geochem. 42 (8), 955-964.

Doolette, A.L., Smernik, R.J., McLaren, T.I., 2017. The composition of organic phosphorus in soils of the Snowy Mountains region of south-eastern Australia. Soil Res. 55, 10-18.

Dougherty, W.J., Smernik, R.J., Bünemann, E.K., Chittleborough, D.J., 2007. On the use of hydrofluoric acid pretreatment of soils for phosphorus-31 nuclear magnetic resonance analyses. Soil Sci. Soc. Am. J. 71 (4), 1111-1118.

George, T.S., Giles, C.D., Menezes-Blackburn, D., Condron, L.M., Gama-Rodrigues, A.C., Jaisi, D., Lang, F., Neal, A.L., Stutter, M.I., Almeida, D.S., Bol, R., Cabugao, K.G., Celi, L., Cotner, J.B., Feng, G., Goll, D.S., Hallama, M., Krueger, J., Plassard, C., Rosling, A., Darch, T., Fraser, T., Giesler, R., Richardson, A.E., Tamburini, F., Shand, C.A., Lumsdon, D.G., Zhang, H., Blackwell, M.S.A., Wearing, C., Mezeli, M.M., Almås, Å.R., Audette, Y., Bertrand, I., Beyhaut, E., Boitt, G., Bradshaw, N., Brearley, C.A., Bruulsema, T.W., Ciais, P., Cozzolino, V., Duran, P.C., Mora, M.L., de Menezes, A.B., Dodd, R.J., Dunfield, K., Engl, C., Frazão, J.J., Garland, G., González Jiménez, J.L., Graca, J., Granger, S.J., Harrison, A.F., Heuck, C., Hou, E.Q., Johnes, P.J., Kaiser, K., Kjær, H.A., Klumpp, E., Lamb, A.L., Macintosh, K.A., Mackay, E.B., McGrath, J., McIntyre, C., McLaren, T., Mészáros, E., Missong, A., Mooshammer, M., Negrón, C.P., Nelson, L.A., Pfahler, V., Poblete-Grant, P., Randall, M., Seguel, A., Seth, K., Smith, A.C., Smits, M.M., Sobarzo, J.A., Spohn, M., Tawaraya, K., Tibbett, M., Voroney, P., Wallander, H., Wang, L., Wasaki, J., Haygarth, P.M., 2018. Organic phosphorus in the terrestrial environment: A perspective on the state of the art and future priorities. Plant Soil 427 (1-2), 191-208.

He, Z., Ohno, T., Cade-Menun, B.J., Erich, M.S., Honeycutt, C.W., 2006. Spectral and chemical characterization of phosphates associated with humic substances Soil Sci. Soc. Am. J. 70 (5), 1741-1751.

Hill, J.E., Cade-Menun, B.J., 2009. Phosphorus-31 nuclear magnetic resonance spectroscopy transect study of poultry operations on the Delmarva peninsula. J. Environ. Qual. 38 (1), 130-138.

IHSS, 2013. Source materials for IHSS samples. International Humic Substances Society.

IUSS Working Group WRB, 2015. World Reference Base for Soil Resources 2014, update 2015 International soil classification system for naming soils and creating legends for soil maps, World Soil Resources Report No. 106. FAO, Rome.

Jarosch, K.A., Doolette, A.L., Smernik, R.J., Tamburini, F., Frossard, E., Bünemann, E.K., 2015. Characterisation of soil organic phosphorus in NaOH-EDTA extracts: A comparison of 31P NMR spectroscopy and enzyme addition assays. Soil Biol. Biochem. 91, 298-309.

Keeler, J., 2010. 9. Relaxation and the NOE. In: J. Keeler (Ed.), Understanding NMR spectroscopy. Wiley, West Sussex, England, pp. 241-317.

Keller, M., Oberson, A., Annaheim, K.E., Tamburini, F., Mäder, P., Mayer, J., Frossard, E., Bünemann, E.K., 2012. Phosphorus forms and enzymatic hydrolyzability of organic phosphorus in soils after 30 years of organic and conventional farming. J. Plant Nutr. Soil Sci. 175 (3), 385-393.

Kirkby, C.A., Kirkegaard, J.A., Richardson, A.E., Wade, L.J., Blanchard, C., Batten, G., 2011. Stable soil organic matter: A comparison of C:N:P:S ratios in Australian and other world soils. Geoderma 163 (3–4), 197-208.

Kouno, K., Tuchiya, Y., Ando, T., 1995. Measurement of soil microbial biomass phosphorus by an anion exchange membrane method. Soil Biol. Biochem. 27 (10), 1353-1357.

Lang, F., Krüger, J., Amelung, W., Willbold, S., Frossard, E., Bünemann, E.K., Bauhus, J., Nitschke, R., Kandeler, E., Marhan, S., Schulz, S., Bergkemper, F., Schloter, M., Luster, J., Guggisberg, F., Kaiser, K., Mikutta, R., Guggenberger, G., Polle, A., Pena, R., Prietzel, J., Rodionov, A., Talkner, U., Meesenburg, H., von Wilpert, K., Hölscher, A., Dietrich, H.P., Chmara, I., 2017. Soil phosphorus supply controls P nutrition strategies of beech forest ecosystems in Central Europe. Biogeochemistry 136 (1), 5-29.

Levitt, M.H., 2008. 12. Experiments on non-interacting spins-1/2. In: M.H. Levitt (Ed.), Spin dynamics: Basics of nuclear magnetic resonance. Wiley, West Sussex, Enlgand, pp. 295-317.

Matejovic, I., 1997. Determination of carbon and nitrogen in samples of various soils by the dry combustion. Commun. Soil Sci. Plant Anal. 28 (17-18), 1499-1511.

McDowell, R.W., Stewart, I., Cade-Menun, B.J., 2006. An examination of spin–lattice relaxation times for analysis of soil and manure extracts by liquid state phosphorus-31 nuclear magnetic resonance spectroscopy. J. Environ. Qual. 35 (1), 293-302.

McKeague, J.A., Day, J.H., 1966. Dithionite- and oxalate-extractable Fe and Al as aids in differentiating various classes of soils. Can. J. Soil Sci. 46 (1), 13-22.

McLaren, T.I., Smernik, R.J., Guppy, C.N., Bell, M.J., Tighe, M.K., 2014. The organic P composition of Vertisols as determined by 31P NMR spectroscopy. Soil Sci. Soc. Am. J. 78 (6), 1893-1902.

McLaren, T.I., Smernik, R.J., McLaughlin, M.J., McBeath, T.M., Kirby, J.K., Simpson, R.J., Guppy, C.N., Doolette, A.L., Richardson, A.E., 2015a. Complex forms of soil organic phosphorus – a major component of soil phosphorus. Environ. Sci. Technol. 49 (22), 13238–13245.

McLaren, T.I., Smernik, R.J., Simpson, R.J., McLaughlin, M.J., McBeath, T.M., Guppy, C.N., Richardson, A.E., 2015b. Spectral sensitivity of solution 31P NMR spectroscopy is improved by narrowing the soil to solution ratio to 1:4 for pasture soils of low organic P content. Geoderma 257-258, 48-57.

McLaren, T.I., Smernik, R.J., Simpson, R.J., McLaughlin, M.J., McBeath, T.M., Guppy, C.N., Richardson, A.E., 2017. The chemical nature of organic phosphorus that accumulates in fertilized soils of a temperate pasture as determined by solution 31P NMR spectroscopy. J. Plant Nutr. Soil Sci. 180 (1), 27-38.

Meiboom, S., Gill, D., 1958. Modified spin-echo method for measuring nuclear relaxation times. Rev. Sci. Instrum. 29 (8), 688-691.

Missong, A., Bol, R., Willbold, S., Siemens, J., Klumpp, E., 2016. Phosphorus forms in forest soil colloids as revealed by liquid-state 31P-NMR. J. Plant Nutr. Soil Sci. 179 (2), 159-167.

Newman, R.H., Tate, K.R., 1980. Soil phosphorus characterisation by 31P nuclear magnetic resonance. Commun. Soil Sci. Plant Anal. 11 (9), 835-842.

506 Noack, S.R., McLaughlin, M.J., Smernik, R.J., McBeath, T.M., Armstrong, R.D., 2012. Crop residue
507 phosphorus: speciation and potential bio-availability. Plant Soil 359 (1-2), 375-385.
508 Ohno, T., Zibilske, L.M., 1991. Determination of low concentrations of phosphorus in soil extracts
509 using malachite green. Soil Sci. Soc. Am. J. 55 (3), 892-895.
510 R Core Team, 2016. R: A language and environment for statistical computing. R Foundation for
511 Statistical Computing, Vienna, Austria.
512 Saunders, W.M.H., Williams, E.G., 1955. Observations on the determination of total organic
513 phosphorus in soils. J. Soil Sci. 6 (2), 254-267.
514 Schefe, C.R., Barlow, K., Robinson, N., Crawford, D., McLaren, T.I., Smernik, R.J., Croatto, G.,
515 Walsh, R., Kitching, M., 2015. 100 Years of superphosphate addition to pasture in an acid soil
516 - current nutrient status and future management. Soil Res. 53 (6), 662-676.
517 Schmidt, M.W.I., Torn, M.S., Abiven, S., Dittmar, T., Guggenberger, G., Janssens, I.A., Kleber, M.,
518 Kögel-Knabner, I., Lehmann, J., Manning, D.A.C., Nannipieri, P., Rasse, D.P., Weiner, S.,
519 Trumbore, S.E., 2011. Persistence of soil organic matter as an ecosystem property. Nature
520 478, 49-56.
521 Schmidt-Rohr, K., Spiess, H.W., 1994. Chapter 3 - High-resolution NMR techniques for solids. In: K.
522 Schmidt-Rohr, H.W. Spiess (Eds.), Multidimensional solid-state NMR and polymers.
523 Academic Press Limited, San Diego, United States, pp. 69-134.
524 Smernik, R.J., Dougherty, W.J., 2007. Identification of phytate in phosphorus-31 nuclear magnetic
525 resonance spectra: The need for spiking. Soil Sci. Soc. Am. J. 71 (3), 1045-1050.
526 Soil Survey Staff, 1992. Keys to Soil Taxonomy. SMSS Technical Monograph, Blacksburg, VA.
527 Spain, A.V., Tibbett, M., Ridd, M., McLaren, T.I., 2018. Phosphorus dynamics in a tropical forest soil
528 restored after strip mining. Plant Soil 427 (1), 105-123.
529 Steward, J.H., Tate, M.E., 1971. Gel chromatography of soil organic phosphorus. J. Chromatogr. A 60,
530 75-82.
531 Swift, R.S., Posner, A.M., 1972. Nitrogen, phosphorus and sulphur contents of humic acids
532 fractionated with respect to molecular weight. J. Soil Sci. 23 (1), 50-57.
533 Thomas, R.L., Bowman, B.T., 1966. The occurrence of high molecular weight organic phosphorus
534 compounds in soil. Soil Sci. Soc. Am. J. 30 (6), 799-801.

Turner, B.L., Mahieu, N., Condron, L.M., 2003. Quantification of *myo*-inositol hexakisphosphate in alkaline soil extracts by solution 31P NMR spectroscopy and spectral deconvolution. Soil Sci. 168 (7), 469-478.

Turner, B.L., Papházy, M.J., Haygarth, P.M., Mckelvie, I.D., 2002. Inositol phosphates in the environment. Philos. Trans. R. Soc. Lond. B Biol. Sci. 357 (1420), 449-469.

van Beek, J.D., 2007. matNMR: A flexible toolbox for processing, analyzing and visualizing magnetic resonance data in Matlab®. Journal of Magnetic Resonance 187 (1), 19-26.

Vestergren, J., Vincent, A.G., Jansson, M., Persson, P., Ilstedt, U., Gröbner, G., Giesler, R., Schleucher, J., 2012. High-resolution characterization of organic phosphorus in soil extracts using 2D 1H–31P NMR correlation spectroscopy. Environ. Sci. Technol. 46 (7), 3950-3956.

Vincent, A.G., Schleucher, J., Gröbner, G., Vestergren, J., Persson, P., Jansson, M., Giesler, R., 2012. Changes in organic phosphorus composition in boreal forest humus soils: the role of iron and aluminium. Biogeochemistry 108 (1-3), 485-499.

Vold, R.L., Waugh, J.S., Klein, M.P., Phelps, D.E., 1968. Measurement of spin relaxation in complex systems. J. Chem. Phys. 48 (8), 3831-3832.

Wang, L., Amelung, W., Willbold, S., 2017. Diffusion-ordered nuclear magnetic resonance spectroscopy (DOSY-NMR): A novel tool for identification of phosphorus compounds in soil extracts. Environ. Sci. Technol. 51 (22), 13256-13264.

555 **List of Figures**

556

557 **Fig. 1.** Solution ^{31}P nuclear magnetic resonance (NMR) spectra obtained with a Carr-Purcell-
558 Meiboom-Gill (CPMG) pulse sequence at a spin-echo delay of 5 ms (black line) and 400 ms (blue line)
559 of the orthophosphate and phosphomonoester region on four soil extracts. Chemical shift (δ, ppm) is
560 reported for the x-axis. The spectra at both spin-echo delays are normalised to the *scyllo*-inositol
561 hexakisphosphate (*scyllo*-IHP) peak, and then the vertical scale of each soil adjusted to highlight
562 spectral features. Identified peaks from orthophosphate, *myo*-inositol hexakisphosphate (*myo*-IHP) and
563 *scyllo*-IHP are indicated with green, red and orange circles, respectively.

564

565

566 **Tables**

567

568 **Table 1.** Some basic chemical properties of the soils used in this study.

Soil parameter	BBR	DOK	VES	Elliot
pH ($BaCl_2$, 1:2)	3.5	6.4	3.3	6.8
Total carbon[a] (g kg^{-1})	88	16	63	51.7
Total nitrogen[a] (g kg^{-1})	6.3	1.6	3.9	4.9
Oxalate aluminium[b] (g kg^{-1})	26.6	2.5	3.9	11.1
Oxalate iron[b] (g kg^{-1})	86.3	8.8	10.1	22.0
Resin P[c] (mg kg^{-1})	19	11	22	22
NaOH-EDTA Total P[d] (mg kg^{-1})	1612	377	730	309
NaOH-EDTA MRP[d] (mg kg^{-1})	613	120	242	86
NaOH-EDTA MUP[d] (mg kg^{-1})	999	258	489	223
Ignition-H_2SO_4 Total P[e]	2614	653	894	550
Ignition-H_2SO_4 Inorganic P[e]	943	276	258	127
Ignition-H_2SO_4 Organic P[e]	1672	378	636	424
Total soil P[f] (mg kg^{-1})	3793	1345	1925	1202

569 [a] Based on the method of Matejovic (1997). [b] Based on the method of McKeague and Day (1966). [c]
570 Based on the method of Kouno et al. (1995). [d] Based on the method of Cade-Menun et al. (2002).
571 Concentrations of total P in NaOH-EDTA extracts were measured by inductively coupled plasma–
572 optical emission spectroscopy (ICP-OES), whereas that of molybdate reactive P (MRP) in NaOH-
573 EDTA extracts were measured colorimetrically, based on Ohno and Zibilske (1991). The difference
574 between total P and MRP in NaOH-EDTA extracts is termed molybdate unreactive P (MUP). [e] Based
575 on the ignition-H_2SO_4 extraction technique of Saunders and Williams (1955). [f] Based on laboratory X-
576 ray fluorescence (LXRF). All measures were carried out on dried soil samples.

577

578

579 **Table 2.** Longitudinal relaxation (T_1) times (s) of the added methylenediphosphonic acid (MDP) and
580 orthophosphate in NaOH-EDTA soil extracts based on solution ^{31}P nuclear magnetic resonance (NMR)
581 spectroscopy with an inversion recovery experiment (Vold et al., 1968). Recycle delay equals the T_1
582 time multiplied by five.

Compound	**BBR**	**DOK**	**VES**	**Elliot**
MDP	0.60	1.40	1.12	1.46
Orthophosphate	0.90	3.89	2.16	4.12

583

584

585 **Table 3.** The transverse relaxation (T_2) times (ms) of various P species based on solution ^{31}P nuclear magnetic resonance (NMR) spectroscopy combined with a Carr-Purcell-

586 Meiboom-Gill (CPMG) pulse sequence on four soil extracts. Values in parentheses are the standard error of the model coefficient.

Chemical compound	**δ ppm**	**BBR**	**DOK**	**VES**	**Elliot**
2-Aminoethylphosphonate	20.0 to 19.8	13.2 (1.8)	–	63.1 (20.7)	–
Unknown phosphonate 1	18.5 to 18.0	–	–	45.4 (14.3)	–
Methylenediphosphonic acid	17.3 to 16.3	10.6 (0.2)	52.6 (3.3)	40.7 (1.5)	46.7 (1.1)
Phosphodiesters (including DNA)	-0.6 to -1.6	12.5 (1.9)	–	13.3 (1.5)	–
Pyrophosphate	-4.3 to -4.6	18.9 ((2.6)	71.1 (13.9)	60.8 (14.1)	53.7 (10.2)
Orthophosphate	5.613	14.0 (0.5)	71.4 (7.0)	46.2 (3.0)	96.8 (12.9)
Phosphomonoesters					
scyllo-IHP	3.340	45.2 (3.1)	67.6 (9.2)	78.0 (13.2)	94.2 (17.8)
myo-IHP (C5)	3.683	40.5 (6.2)	–	60.6 (5.6)	–
myo-IHP (C1, C3)	3.803	32.1 (1.1)	72.9 (11.6)	57.1 (1.15)	–
myo-IHP (C4, C6)	4.192	37.3 (6.7)	70.7 (22.8)	65.6 (6.1)	–
myo-IHP (C2)	5.116	37.8 (4.8)	45.6 (14.1)	52.3 (3.7)	–
myo-IHP (combined)	–	35.8 (2.4)	67.6 (12.8)	59.0 (2.3)	–
Broad signal	–	20.4 (1.2)	26.8 (2.6)	42.6 (2.1)	31.8 (2.7)

587

588

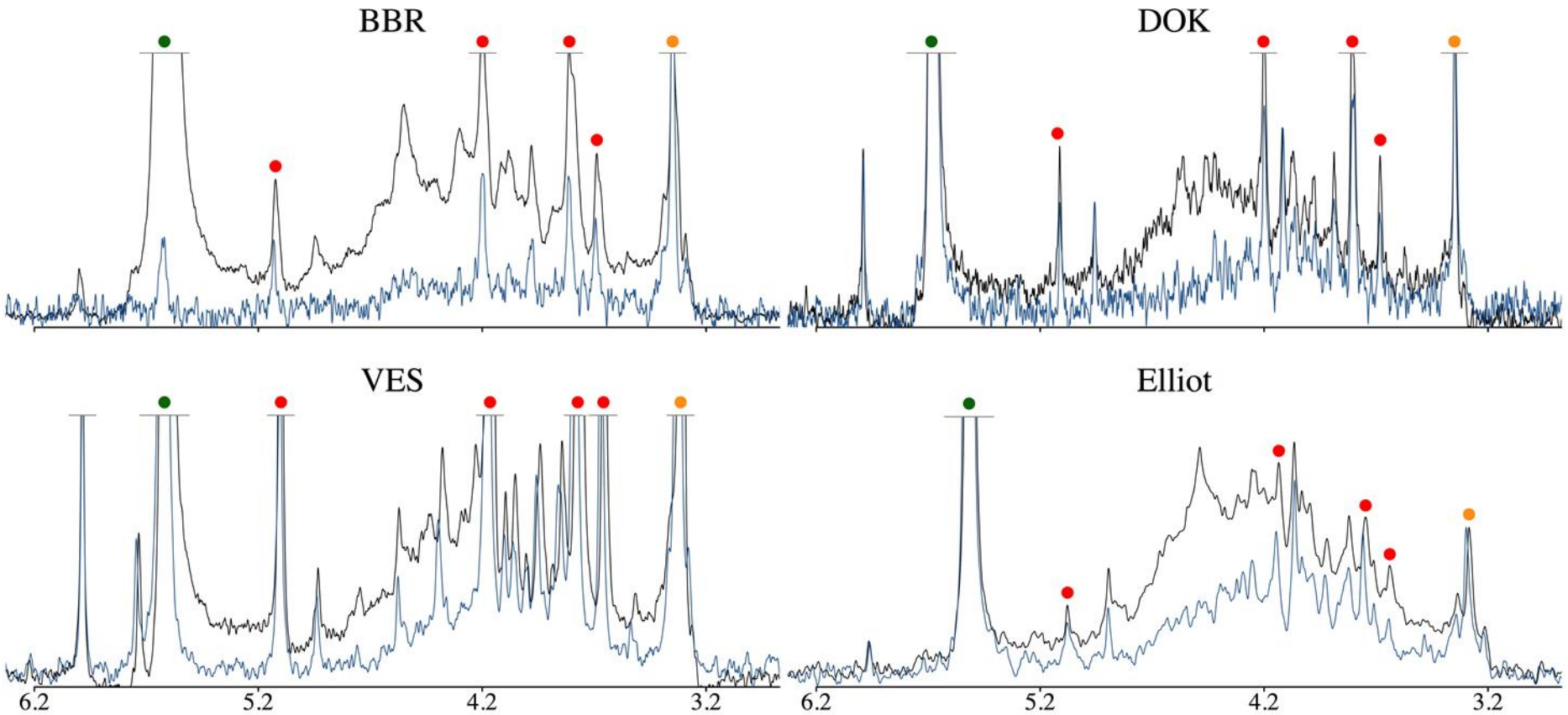

589
590 **Figure 1.** Solution ^{31}P nuclear magnetic resonance (NMR) spectra obtained with a Carr-Purcell-Meiboom-Gill (CPMG) sequence at a spin-echo delay of 5 ms (black line)
591 and 400 ms (blue line) of the orthophosphate and phosphomonoester region on four soil extracts. Chemical shift (δ, ppm) is reported for the x-axis. The spectra at both spin-
592 echo delays are normalised to the *scyllo*-inositol hexakisphosphate (*scyllo*-IHP) peak, and then the vertical scale of each soil adjusted to highlight spectral features. Identified
593 peaks from orthophosphate, *myo*-inositol hexakisphosphate (*myo*-IHP) and *scyllo*-IHP are indicated with green, red and orange circles, respectively.

594